Molecular-dynamics study of long-lived structures in a fragile glass-forming liquid

Gregory Johnson,[1] Andrew I. Mel'cuk,[2] Harvey Gould,[1] W. Klein,[3] and Raymond D. Mountain[4]

[1]*Department of Physics, Clark University, Worcester, Massachusetts 01610*
[2]*Polymer Science and Engineering Department, University of Massachusetts, Amherst, Massachusetts 01002*
[3]*Department of Physics, Boston University, Boston, Massachusetts 02215*
[4]*Physical and Chemical Properties Division, National Institute of Standards and Technology, Gaithersburg, Maryland 20899*

We present molecular-dynamics results for a two-component, two-dimensional Lennard-Jones supercooled liquid near the glass transition. We find that the supercooled liquid is spatially heterogeneous and that there are long-lived clusters whose size distribution satisfies a scaling relation up to a cutoff. The similarity of several properties of the supercooled liquid to those of a mean-field glass-forming fluid near the spinodal suggests that the glass transition in the supercooled liquid is associated with an underlying thermodynamic instability. [S1063-651X(98)00505-4]

PACS number(s): 64.70.Pf, 61.43.Fs, 61.20.Lc

I. INTRODUCTION

The characterization of supercooled liquids near the glass transition is an active area of research [1]. Outstanding unsolved problems include the possible existence of an underlying thermodynamic glass transition, the history dependence of the glass properties, and the mechanisms responsible for the large increase in relaxation times as the glass transition is approached. In this article we discuss our molecular-dynamics simulations of a two-component, two-dimensional ($d=2$) Lennard-Jones supercooled liquid. A summary of some of our results has been published earlier [2].

To help the reader understand our interpretation of the molecular-dynamics data and the questions we pose, we first review the behavior of a mean-field model of a structural glass transition [3]. In the mean-field model, particles interact via a repulsive, two-body potential of the form [4] $V(r) = \gamma^d \phi(\gamma r)$, where r is the interparticle distance and d is the spatial dimension. The range of the interaction is $R = \gamma^{-1}$. In the limit $R \to \infty$, the static properties of the uniform fluid are described exactly by mean-field theory [4]. The equilibrium structure function $S(k)$ can be shown to satisfy the Ornstein-Zernicke form, $S(k) = 1/[1 + \beta \rho \hat{\phi}(k)]$, where ρ is the particle density, $\beta^{-1} = k_B T$, and $\hat{\phi}(k)$ is the Fourier transform of $\phi(x)$. We choose the step potential, $\phi(x) = 1$ for $x \leq 1$ and $\phi(x) = 0$ for $x > 1$. The Fourier transform $\hat{\phi}(k)$ is negative for various values of k. This property of $\hat{\phi}(k)$ implies that in the mean-field limit, $S(k)$ becomes negative in some range of k for sufficiently large $\beta \rho$. Hence for fixed ρ, the system has a spinodal singularity [5] at a temperature $T = T_s$ which is defined by the condition $1 + \beta_s \rho \hat{\phi}(k_0) = 0$, where k_0 is the location of the minimum of $\hat{\phi}(k)$. At $T = T_s$, $S(k)$ diverges at k_0; for $T > T_s$, $S(k_0)$ diverges as $(T - T_s)^{-\gamma}$ with the mean-field exponent $\gamma = 1$. Note that the spinodal is the limit of thermodynamic stability of the uniform phase and is a critical point (for a given density). However, unlike the usual critical point, the structure function diverges at a nonzero value of k.

For $d = 3$ and $\rho = 1.95$, the spinodal is at $T_s = 0.705$ ($k_B = 1$) [3]. Although the singularity is well defined only in the mean-field limit, simulations must be done for finite R. Monte Carlo simulations for $R = 3$ with $\rho = 1.95$ yield a $S(k)$ which has a maximum at $k \neq 0$ that increases rapidly as T is decreased until $T \approx 0.75$, below which the peak ceases to increase as T is lowered [3,6]. This behavior is characteristic of a pseudospinodal [7].

One way of understanding the simulation results for $S(k)$ is to interpret the spinodal as a singularity of the free energy as a function of T, ρ. If the interaction range is finite, the singularity is in the four-dimensional complex (T, ρ) plane as has been found in transfer matrix studies of long-range ferromagnetic Ising models [8]. The singularity moves closer to the real axis as the range of interaction increases. We refer to the complex singularity in finite-range systems as a pseudospinodal. The physical effects of the pseudospinodal depend on how far it is from the real axis. As R increases, the pseudospinodal better approximates a true singularity and has measurable effects if R is sufficiently large.

The fact that the mean-field model has a spinodal is unambiguous. We now discuss the reasons why we can associate the spinodal with a thermodynamic glass transition. In the Monte Carlo simulation for fixed ρ we equilibrate the system at a high $T > T_s$ where the uniform phase is stable and then quench it to $T < T_s$ where the uniform phase is unstable. After the quench the particles immediately form clumps with order ρR^3 particles in each clump [6]. That is, the system breaks up into regions of high particle density surrounded by regions of low particle density. The arrangement of the clumps is noncrystalline and their number depends on the quench history [3,6]. The free energy has been calculated numerically in the mean-field limit and has many minima corresponding to different numbers of clumps [3,9]. For $T < T_s$, the system remains trapped in a local free energy minimum. The minimum the system chooses appears to depend on the quench history.

The multiminima free energy and the quench history dependence suggest that the mean-field model has a metastable glass phase for $T < T_s$. However, the properties of a glass are associated more with its dynamical properties. As we will discuss, the glassy dynamics of the mean-field model is as-

sociated with the behavior of the *clumps*; the *particles* are not localized in the metastable glass phase. That is, the dynamical properties associated with single particle behavior do not show the usual signature of the approach to a glass. A simple argument based on the fact that all potential barriers in the mean-field model are finite [2] implies that the self-diffusion coefficient D is nonzero for all $T > 0$. Hence, if the observation time is sufficiently long, the mean square displacement of the particles increases indefinitely. The argument proceeds as follows. Because the separation between the clumps is order R, the interaction of the particles in a particular clump with the particles in neighboring clumps is minimized. Inside a clump, a particle undergoes a restricted random walk. A particle that attempts to leave a clump experiences a potential barrier due to the proximity of other clumps. Such a particle must interact with particles in the same clump and with particles in at least one other clump at some time during its possible escape. The upper bound of the potential barrier is $c \gamma^d R^d$, where the constant c depends on d. (Recall that γ^d is the strength of the interaction and R^d is proportional to the number of particles in a clump such that $\gamma^d R^d = 1$.) The probability of leaving a clump in a Monte Carlo simulation is bounded from below by $\frac{1}{2} e^{-c/k_B T}$ for all R and hence $D > 0$. Similar arguments hold for a molecular-dynamics simulation of the same system.

The same argument implies that the mean-field model is ergodic for all $T > 0$ if single particle properties are probed. The ergodic behavior can be characterized by several fluctuation metrics [10]. The single particle energy fluctuation metric $\Omega_\epsilon(t)$ is given by [10]

$$\Omega_\epsilon(t) = \frac{1}{N} \sum_{i=1}^{N} [\bar{\epsilon}_i(t) - \langle \bar{\epsilon}(t) \rangle]^2, \qquad (1)$$

where

$$\bar{\epsilon}_i(t) = \frac{1}{t} \int_0^t \epsilon_i(t') \, dt' \qquad (2)$$

is the energy of particle i averaged over the time interval t, and $\langle \bar{\epsilon}(t) \rangle = (1/N) \Sigma_{i=1}^{N} \bar{\epsilon}_i(t)$. The single particle energy ϵ_i of particle i includes its kinetic energy and one-half of the potential energy of its interaction with other particles in the system. If the system is ergodic, $\Omega_\epsilon(t) \sim 1/t$ for t sufficiently large [10]. We find that $\Omega_\epsilon(t)$ exhibits ergodic behavior at $T = 0.4$, a value of $T < T_s$. However, for $T \lesssim 0.15$, $1/\Omega_\epsilon(t)$ is not proportional to t during our longest runs, and the measured D is indistinguishable from zero at $T = 0.15$. Given our theoretical argument that D is nonzero for all $T > 0$, the observed behavior of $1/\Omega_\epsilon(t)$ for $T < 0.15$ implies only that the time for a particle to leave a clump is much longer than our observation time. We interpret this change from ergodic to nonergodic behavior as an apparent kinetic transition.

How can we reconcile the T dependence of D and $\Omega_\epsilon(t)$ with our identification of T_s as the spinodal-glass transition? The answer lies in the dynamical properties of the *clumps*. For example, the diffusion coefficient of the center of mass of the clumps, D_{cl}, is zero for $T < T_s$ in the mean-field limit. To understand this behavior, note that n_{cl}, the mean number of particles in a clump, diverges as R^d as $R \to \infty$. In this limit,

the number of clumps does not change with time and the mean numbers of particles exiting and entering a clump are equal. From the central limit theorem, the relative fluctuations of these quantities go to zero as R and $n_{cl} \to \infty$. We conclude that $D_{cl} \lesssim D/\sqrt{n_{cl}}$, and hence $D_{cl} = 0$ in the mean-field limit. Our simulations of D_{cl} for finite R are consistent with this prediction, and also indicate that the clumps are not affected by the same local environment, that is, they have different numbers of nearest neighbor clumps. This difference in the local environment persists as $R \to \infty$ because the clumps do not diffuse and cannot sample different local environments. Hence, the system is nonergodic on a clump (mass $\sim R^d$) scale for $T < T_s$ in the mean-field limit.

In summary, the static properties of the mean-field glass phase are dominated by localized, long-lived structures (clumps) for $T < T_s$, even though particles move from clump to clump. The time scale for the motion of the clumps diverges in the mean-field limit, and the spinodal-glass transition is seen dynamically only on a clump scale. However, we observe an *apparent* kinetic transition that is associated with the slow diffusion of the particles and the finite duration of our runs. The temperature of this apparent transition is less than T_s and depends on the observation time.

The well characterized behavior of the mean-field glass model motivates us to ask if similar behavior occurs in systems with more realistic interactions. In Sec. II we discuss the static properties of a two-component, two-dimensional system of Lennard-Jones particles and find that the system exhibits the usual properties associated with other simulations of glassy systems. In Sec. III we compute the static structure function $S(k)$ and find evidence for a weak divergence in the height of the diffraction peak as T is lowered. This divergence is interpreted as evidence for the influence of a pseudospinodal. In Sec. IV we propose a criterion for clusters of solidlike particles and find evidence of cluster scaling and an ergodic to nonergodic transition in the dynamics of the clusters. In Sec. V we discuss the interpretation of our molecular-dynamics results in terms of a mean-field perspective.

II. LENNARD-JONES MODEL

Because it is easier to identify geometrical structures in two dimensions than in three, we consider a two-dimensional system. We also specify that the particles interact via a Lennard-Jones potential because of the extensive simulations of supercooled Lennard-Jones liquids. However, a single-component, two-dimensional Lennard-Jones system quickly nucleates to a solid and is unlikely to form a glasslike state. We follow Wong and Chester [11], who have done a Monte Carlo study of the quenched states of two-component, two-dimensional Lennard-Jones systems with the goal of choosing the density and the size of the minority component so that it inhibits nucleation of the majority component to a solid.

We designate by V_{ab} the interaction between a particle belonging to species a and a particle belonging to species b and write $V_{ab} = 4\epsilon[(\sigma_{ab}/r)^{12} - (\sigma_{ab}/r)^6]$. We follow Ref. [11] and choose $\sigma_{aa} = \sigma$, $\sigma_{bb} = 3\sigma/2$, and $\sigma_{ab} = \frac{1}{2}(\sigma_{aa} + \sigma_{bb}) = 5\sigma/4$. The energy parameter ϵ and the mass m are the same for both species. The Lennard-Jones potential is cut

TABLE I. Values of the mean temperature T, the mean pressure P, the height of the first peak of the radial distribution function $g(r)$, and the height $\chi(k_0)$ and width $w(k_0)$ of the diffraction peak of the static structure function $S(k)$ averaged over runs of $100\,000\tau$ each. The mean pressure was computed from the virial. The width of the first peak of $g(r)$ does not appear to change with T and is not listed. The density ρ is fixed at $\rho=0.952$. As stated in the text, the lowest temperature run is probably not in complete thermal equilibrium.

T	P	$g(r_{\mathrm{max}})$	$\chi(k_0)$	$w(k_0)$
5.5	91.1	4.30	2.59	1.11
4.6	85.3	4.54	2.70	0.95
3.7	77.8	4.91	2.87	0.87
3.3	74.9	5.15	3.10	0.76
3.1	72.9	5.33	3.49	0.63
2.7	69.0	5.68	4.28	0.45
2.5	67.3	5.86	3.94	0.55
2.25	65.0	6.07	3.54	0.54

off at $r=2.5\sigma_{ab}$ and shifted so that the potential is to zero at the cutoff. We choose units such that lengths are measured in terms of σ, energies in terms of ϵ, and the time in terms of $\tau=(m\sigma^2/\epsilon)^{1/2}$. For example, the reduced number density is $\rho^*=\rho\sigma^2$. In the following, we will omit the asterisk and quote all results in reduced units. Because the time can be expressed either in terms of the number of time steps or in terms of τ, we will explicitly specify the units of time.

The majority a component is taken to be 80% of the total number of particles N. All but one of the simulations are for $N=500$. This relatively small number of particles was chosen so that long runs could be made. The duration of the run for each temperature was $100\,000\tau$ unless otherwise noted. The molecular-dynamics simulations were performed with periodic boundary conditions at constant energy and volume [12] at a density of $\rho=0.952$, corresponding to $L=22.92$, where L is the linear dimension of the simulation cell. We used the velocity form of the Verlet algorithm [12] with a time step of $\Delta t=0.005\tau$ for all temperatures except for $T=5.5$ for which we choose $\Delta t=0.0025\tau$ to achieve reasonable energy conservation. The mean temperatures and pressures of our eight different runs are shown in Table I. As a typical example of the statistical accuracy of these mean values, we note that the run at $T=3.1$ corresponds to a mean temperature of 3.15 over the first $50\,000\tau$ and 3.13 over the second $50\,000\tau$. However for $T=2.25$, the mean temperatures were 2.21 and 2.29, respectively, and it is possible that the lowest temperature run has not reached thermal equilibrium.

Because our results are for constant density rather than constant pressure, the values of various quantities to be discussed here will differ slightly from our earlier results cited in Ref. [2] which were for a pressure of $P\approx70$ and different densities. The initial configuration of each run at a particular temperature was the final configuration obtained previously [2,13]. In some cases the positions had to be rescaled to obtain the desired density. Unless otherwise stated, the system was allowed to equilibrate for at least $50\,000\tau$ and then data were collected for $100\,000\tau$. This duration is one to two orders of magnitude longer than reported previously [2]
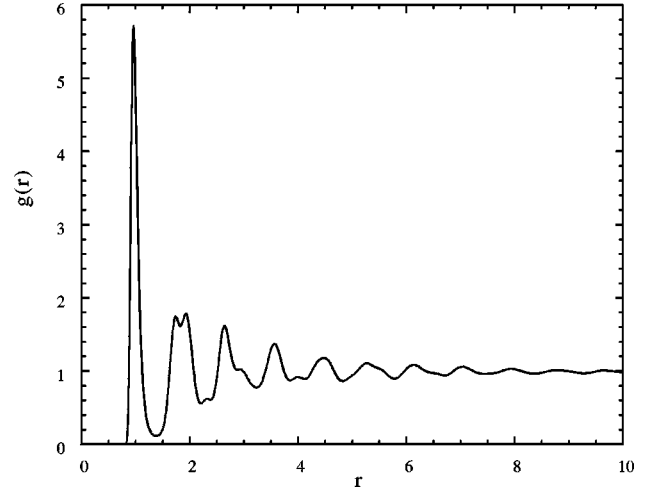

FIG. 1. Plot of the radial distribution function $g(r)$ versus r at $T=2.7$. Note the split second peak, a possible signature of a glassy state. Only the small, majority particles were included. The dimensionless quantity r is measured in terms of the Lennard-Jones parameter σ.

and is equivalent to runs of approximately 2×10^{-7} s for liquid argon.

We first compute the radial distribution function $g(r)$ and the self-diffusion coefficient D and show that they exhibit behavior similar to that found in other simulations of supercooled liquids. All of the following results are for the majority particles only unless otherwise noted. The positions of the particles were saved every 5τ and $g(r)$ was computed in a separate program. In Fig. 1 we show $g(r)$ for $T=2.7$. Note the split second peak, a possible signature of a glassy state [11]; the split second peak of $g(r)$ is not observed for $T>3.1$. The increase in the height of the first peak of $g(r)$ as the temperature is lowered (see Table I) indicates the growth of short-range order. We discuss the temperature dependence of the enthalpy and the constant pressure heat capacity in the Appendix.

The single particle self-diffusion coefficient D is related to the mean square displacement $R^2(t)$ by $\lim_{t\to\infty}R^2(t)=2dDt$. An alternative way of determining D is from the velocity fluctuation metric $\Omega_v(t)$ defined as [10]

$$\Omega_v(t)=\frac{1}{N}\sum_{i=1}^{N}\frac{1}{d}\sum_{\alpha=1}^{d}[\bar{v}_{i,\alpha}(t)-\langle\bar{v}_\alpha(t)\rangle]^2, \qquad (3)$$

where $v_{i,\alpha}$ is the α component of the velocity $\mathbf{v}_i$ of particle i. The time average, $\bar{v}_{i,\alpha}(t)$, of $v_{i,\alpha}$ is defined as in Eq. (2) and the quantity $\langle\bar{v}_\alpha(t)\rangle$ is the average of $\bar{v}_{i,\alpha}(t)$ over all particles. In our simulations the total momentum of the system is equal to zero, and hence $\langle\bar{v}_\alpha(t)\rangle=0$. Because $\int_0^t\mathbf{v}_i(t')\,dt'=\mathbf{r}_i(t)-\mathbf{r}_i(0)$, we can express $\Omega_v(t)$ as

$$\Omega_v(t)=R^2(t)/2t^2. \qquad (4)$$

If the particles are undergoing diffusion, we have

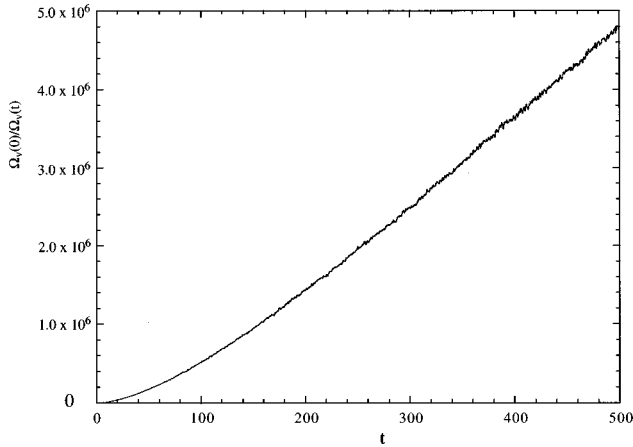$$\Omega_v(t)\to\frac{2D}{t}. \qquad (5)$$

FIG. 2. Plot of $\Omega_v(0)/\Omega_v(t)$, the reciprocal of the velocity fluctuation metric, at $T=2.25$. Note that $1/\Omega_v(t)$ is not linear for $t<250\tau$, but becomes approximately linear for longer times. The temperature T is dimensionless (see text).

The relation (5) was also used to determine D.

For each value of T, the quantity $|\mathbf{r}_i(t+t_0)-\mathbf{r}_i(t_0)|^2$ was computed in a separate program by grouping the particle coordinate data into blocks of duration 500τ and averaging over all possible choices of the origin t_0 and combinations of time differences $t\leqslant250$ for a particular block. The results were then averaged over the 200 blocks. The velocity metric was computed at each time step in the main molecular-dynamics program and the results also were averaged over 200 time origins. The typical time dependence of $\Omega_v(0)/\Omega_v(t)$ is shown in Fig. 2 for $T=2.25$. Note that at this temperature $1/\Omega_v(t)$ is not linear for $t<200\tau$, but becomes linear for longer observation times.

Our results for D obtained from $R^2(t)$ and $1/\Omega_v(t)$ are summarized in Table II. The difference in the values of D determined by the two methods is a measure of the error in the determination of D. In the similar three-dimensional system studied in Ref. [9], $D(T)$ was fit to the Vogel-Fulcher form

$$D(T)=A\ e^{-B/(T-T_0)}, \tag{6}$$

and we look for similar behavior. From the semilog plot of D versus $1/T$ shown in Fig. 3, it is easy to verify that the best

TABLE II. Summary of results for the self-diffusion coefficient D as a function of temperature T at constant density $\rho=0.952$. The second column represents the estimates of D determined from the slope of $R^2(t)$, and the third column gives the estimates of D from the slope of $1/\Omega_v(t)$ [see Eq. (5)].

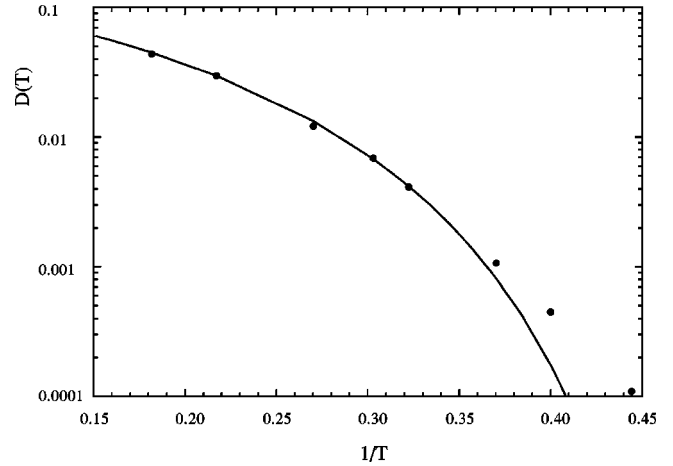| T	D [from $R^2(t)$]	D [from $1/\Omega_v(t)$]
5.5	4.4×10^{-2}	4.8×10^{-2}
4.6	3.0×10^{-2}	3.1×10^{-2}
3.7	1.2×10^{-2}	1.2×10^{-2}
3.3	6.9×10^{-3}	6.8×10^{-3}
3.1	4.1×10^{-3}	4.2×10^{-3}
2.7	1.1×10^{-3}	8.1×10^{-4}
2.5	4.5×10^{-4}	4.2×10^{-4}
2.25	1.1×10^{-4}	6.7×10^{-5}

FIG. 3. Semilog plot of the (dimensionless) self-diffusion coefficient D versus $1/T$. The data points (filled circles) are taken from the second column in Table II. The solid line represents the best fit to the results for D in the interval $2.25\leqslant T\leqslant5.5$ extracted from $R^2(t)$ to the Vogel-Fulcher form $D(T)=Ae^{-B/(T-T_0)}$ with $A=0.16$, $B=4.7$, and $T_0=1.82$.

fits are for $T_0>0$. The best fit for all eight temperatures in Table II occurs for $T_0\approx1.8$ and $T_0\approx1.7$ using the values of D obtained from $R^2(t)$ and $1/\Omega_v(t)$, respectively. However, as shown in Table IV the results for T_0 are sensitive to the number of data points which are included in the least squares fits. The range of reasonable fits illustrates the difficulty of obtaining meaningful values of T_0. We conclude that the temperature dependence of $D(T)$ is consistent with the Vogel-Fulcher form with T_0 in the range $1\leqslant T_0\leqslant2$. Note that the Vogel-Fulcher form of $D(T)$ implies that the system loses ergodicity at $T=T_0$.

We also calculate the single particle energy fluctuation metric $\Omega_\epsilon(t)$ [see Eq. (1)] to see if it exhibits ergodic behavior. If the system is ergodic, we expect that [10]

$$\Omega_\epsilon(t)\rightarrow2\tau_\epsilon/t. \tag{7}$$

We interpret τ_ϵ as the energy mixing time. The energy fluctuation metric was computed ''on the fly'' in the same way as $\Omega_v(t)$, but for a duration of $50\,000\tau$ rather than $100\,000\tau$. We observed that $1/\Omega_\epsilon(t)$ becomes approximately linear even at the lowest temperature $T=2.25$, indicating that the system is ergodic according to this measure. Our results for the T dependence of $\tau_\epsilon(T)$ based on Eq. (7) are summarized in Table III and are plotted in Fig. 4. Note that the largest mixing time is order $10\,000\tau$. For comparison, we also show in Table III the values of $\tau_D=\sigma^2/(4D)$, the mean time it takes a particle to traverse the distance σ. As summarized in Table IV, the fits of $\tau_\epsilon(T)$ to the Vogel-Fulcher form $\tau_\epsilon(T)=A\ e^{-B/(T-T_\epsilon)}$ in different temperature intervals also yields a range of values for the parameter T_ϵ. We conclude that the temperature dependence of τ_ϵ is consistent with the Vogel-Fulcher form with a value of T_ϵ consistent with the value of T_0 determined from the self-diffusion coefficient.

III. EVIDENCE OF PSEUDOSPINODAL BEHAVIOR

Now that we have established that the two-component, two-dimensional supercooled Lennard-Jones system has

TABLE III. Summary of characteristic times. The cluster mixing time τ_{cl} is computed as in Eq. (7) from the cluster metric Ω_{cl}. The single particle time $\tau_D = \sigma^2/(4D)$, the mean time it takes a particle to diffuse a distance σ, and the energy mixing time τ_ϵ from Eq. (7) are shown for comparison. (The values of τ_D are obtained from the second column in Table II.)

T	τ_{cl}	τ_D	τ_ϵ
5.5	5×10^2	5.7	16
4.6	1×10^3	8.4	28
3.7	5×10^3	20	69
3.3	2×10^4	36	140
3.1	5×10^4	60	260
2.7	5×10^5	230	1 100
2.5	5×10^5	560	1 400
2.25		2300	11 000

properties similar to those observed in other simulations of deeply supercooled systems, we explore how the mean-field interpretation discussed in Sec. I is applicable to the present Lennard-Jones system. If the Lennard-Jones system exhibits pseudospinodal effects, we should find behavior analogous to that observed in the mean-field glass model [3] and in Ising models with long-, but finite-range interactions [7]. In these systems, the static structure function $S(k)$ appears to diverge at a nonzero value of k if its behavior is extrapolated from high T or small magnetic field, but the extrapolated singularity is not observed if measurements are made too close to the apparent singularity.

We compute $S(k)$ (for the majority particles) from the saved particle positions using the relation

$$S(k) = \frac{1}{N} \left| \sum_{i=1}^{N} e^{i\mathbf{k} \cdot \mathbf{r}_i} \right|^2. \tag{8}$$

Angular averages were computed by considering all possible k vectors. We calculated $S(k)$ for the same configurations as were used for obtaining $g(r)$. The k dependence of $S(k)$ at $T = 2.7$ is plotted in Fig. 5. Because the number of particles is fixed, we expect that $S(k) \to 1$ as $k \to 0$. The important feature of $S(k)$ is the diffraction peak at $k = k_0 \approx 7.15$. We interpret the height of this peak as a k-dependent susceptibility $\chi(k_0, T)$, and the width $w(k_0, T)$ as an inverse length proportional to the size of the correlated regions in the liquid. These quantities were extracted from $S(k)$ by fitting the region around $k = k_0$ to the four parameter form, $S(k) = a + b/[(k - k_0)^2 + c]$.

Our results for $\chi(k_0, T)$ and $w(k_0, T)$ are listed in Table I and plotted in Fig. 6. Note that $\chi(k_0, T)$ increases by a factor of approximately 1.6 and $w(k_0, T)$ decreases by a factor of approximately 2.0 as T is lowered from 5.5 to 2.5. Because this range of T is limited, we can fit $\chi(k_0, T)$ and $w(k_0, T)$ to a variety of functional forms. Given the divergent behavior of the first peak of $S(k)$ in the mean-field model discussed in Sec. I, we look for fits to the functional forms, $\chi(k_0, T) \sim (T - T_s)^{-\gamma}$ and $w(k_0, T) \sim (T - T_s)^\nu$, where T_s, γ, and ν are fit parameters. We find that the best fit to the assumed power-law form is $\chi(k_0, T) \sim (T - 2.6)^{-0.16}$ and $w(k_0, T) \sim (T - 2.6)^{0.29}$ if results in the interval $2.7 \leq T \leq 4.6$ are in-

cluded. A least squares fit in the interval $3.1 \leq T \leq 5.5$ yields $\chi(k_0, T) \sim (T - 3.0)^{-0.08}$ and $w(k_0, T) \sim (T - 3.0)^{0.19}$. Given the limited range of T, these power-laws fits are justified *only* in the context of our rigorous results for $S(k)$ in the mean-field model [3] for which $\chi(k_0, T) \sim (T - T_s)^{-1}$. The power-law fits suggest that the increase of the height and the decrease in the width of the first peak of $S(k)$ are influenced by a weak singularity at $T = T_s$ with T_s in the range $2.6 \leq T_s \leq 3.0$. As expected, no evidence of a singularity is found if we fit the results for $\chi(k_0, T)$ in the interval $2.25 \leq T \leq 5.5$.

IV. CLUSTER SCALING AND LIFETIME

Given the preliminary pseudospinodal interpretation that we presented in Sec. III, we seek other evidence for the existence of a pseudospinodal and mean-field behavior. For temperatures near the pseudospinodal the system should show signs of an instability and the system should partially phase separate. That is, we should see regions where the majority particles dominate and locally order. For this reason we look for long-lived structures whose constituent particles remain in close proximity to each other over extended times at sufficiently low T. Because of the strong repulsive Lennard-Jones interaction near the origin, these structures will not be identical to the clumps found in the mean-field model, but instead should be caused by a cage effect. A visual examination of the configurations shows evidence of a partial phase separation in which a significant fraction of the majority particles form clusters of triangularlike structures which become better defined as the temperature is decreased. Qualitatively, the lifetime of these visual clusters in the range of temperatures of interest appears to be much longer than the period of oscillation of the particles about their mean position in the clusters.

To find these structures we seek to define a ''solidlike'' particle such that clusters of these particles have the above qualitative properties. However, unlike the Ising model near the critical point [14] and near the spinodal [15], there is no theoretical definition of clusters in a dense liquid, and we
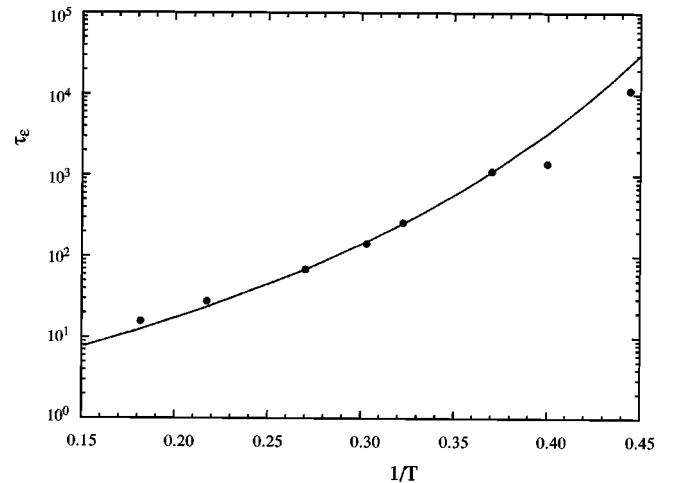

FIG. 4. Semilog plot of the (dimensionless) energy mixing time τ_ϵ defined in Eq. (7) versus $1/T$. The data points (filled circles) are taken from Table III. The solid line represents the best fit to the Vogel-Fulcher form $\tau_\epsilon = A e^{B/(T - T_\epsilon)}$ with $A = 1.24$, $B = 9.8$, and $T_\epsilon = 1.25$ for the six temperatures in the interval $2.7 \leq T \leq 5.5$.

TABLE IV. Range of fits for the temperature parameter T_0 from least squares fits of the self-diffusion coefficient D, the energy mixing time τ_ϵ, and the cluster mixing time T_{cl} to the Vogel-Fulcher form (6).

Temperature interval	T_0 [from $R^2(t)$]	T_0 [from $1/\Omega_v(t)$]
$2.25 \leq T \leq 5.5$	1.82	1.67
$2.7 \leq T \leq 5.5$	1.83	1.21
$2.25 \leq T \leq 4.6$	0.97	1.30
$2.7 \leq T \leq 4.6$	0.94	1.30
	T_ϵ	
$2.25 \leq T \leq 5.5$	no fit	
$2.7 \leq T \leq 5.5$	1.25	
$2.7 \leq T \leq 4.6$	1.25	
$3.1 \leq T \leq 5.5$	1.68	
$3.1 \leq T \leq 4.6$	1.95	
	T_{cl}	
$2.25 \leq T \leq 5.5$	no fit	
$2.7 \leq T \leq 5.5$	1.58	
$2.7 \leq T \leq 4.6$	1.57	
$3.1 \leq T \leq 5.5$	1.58	

have to rely on our physical intuition to define them. We will assume that a cluster consists of a group of solidlike particles and that if two solidlike particles are near neighbors, they belong to the same cluster. Ideally, we would like to introduce a physical property that exhibits bimodal behavior with one peak corresponding to solidlike particles. However, all of the physical quantities we measured exhibit a single peak, and hence we will need to introduce a cutoff to distinguish solidlike and nonsolidlike particles. Nevertheless, we will find that the properties of the resultant clusters do not depend strongly on the choice of cutoff.

Because we are interested in the local environment of the particles, it is natural to do a Voronoi construction [16] and determine the Voronoi polygon of each particle and its Voronoi neighbors. Quantities associated with the Voronoi construction include the distribution of the number of edges of the Voronoi polygons, the distribution of the area of the polygons, and the distribution of the length of the sides. For our two-dimensional system, the mean number of edges of the Voronoi polygons is six and the distribution of the number of edges is temperature independent. This independence is expected because the Voronoi construction in two dimensions is insensitive to thermal fluctuations [13].

To quantify the temperature-dependent changes in the distribution of lengths of the sides of the Voronoi polygons with six sides, we introduce the standard deviation σ_ℓ of the edge length of a particular particle as [17]

$$\sigma_\ell^2 = \langle \ell^2 \rangle - \langle \ell \rangle^2, \qquad (9)$$

where $\langle f(\ell) \rangle = (1/6)\Sigma_{\alpha=1}^6 f(\ell_\alpha)$ and ℓ_α is the length of edge α of the hexagon of interest. If a particle were in a perfect triangular environment, then $\sigma_\ell = 0$. In Fig. 7 we show the estimated probability density $P(h)$ of the quantity $h = \sigma_\ell^2/\langle \ell \rangle^2$, a measure of the "hexagonality" of the poly-

gons. At $T=5.5$, the Voronoi polygons are irregular, giving rise to a high percentage of particles with $h>0.1$. At $T=2.7$, the most probable value of h is at $h=0.014$, and many more particles have regular Voronoi polygons.

In the following, we define a majority particle to be solidlike if it has six Voronoi neighbors and if the condition $h \leq 0.1$ is satisfied. The choice of the cutoff parameter is not crucial and the qualitative properties of the clusters are *independent* of the cutoffs over a wide range of values [13]. A typical configuration of the system at $T=3.3$ is shown in Fig. 8.

Given our criteria for solidlike particles and our definition of clusters, we can determine the properties of the clusters. A separate program using a Voronoi construction and a Hoshen-Kopelman cluster labeling algorithm was used to determine the clusters. Because the height of the maximum of $S(k)$ increases and the width of the peak decreases as T is lowered, we expect that the mean size of the clusters grows as T is lowered until their growth becomes "frustrated" by the presence of the larger minority component and by the different orientations of the other clusters. (The size of a cluster is its number of particles.) The behavior of the cluster size distribution n_s as a function of the size s is plotted in Fig. 9 for $T=3.3$ and $N=500$. The cluster distribution is normalized by the number of (majority) particles so that n_s is the probability that a particle belongs to a cluster of size s. The results for n_s are averaged over $100\,000\tau$. We expect that the presence of a pseudospinodal leads to power-law scaling of the clusters if T is close, but not too close to the pseudospinodal, that is, we expect $n_s \sim s^{-x}$ for a range of values of s. The lack of a true spinodal should lead to a cutoff or lack of scaling for large clusters or for temperatures far from the pseudospinodal. From the log-log plot of n_s versus s in Fig. 9 we see that the s dependence of n_s is consistent with a power-law dependence with an exponent of $x \approx 1.8$ over approximately one decade of s.

The behavior of n_s for lower temperatures is qualitatively different. For example, compare the behavior of n_s averaged over the first $50\,000\tau$ of the run at $T=3.1$ to the plot of n_s averaged over the second $50\,000\tau$ of the run (see Fig. 10). The difference in the cluster size distribution for larger values of s indicates that the lifetime of the clusters at $T=3.1$ is
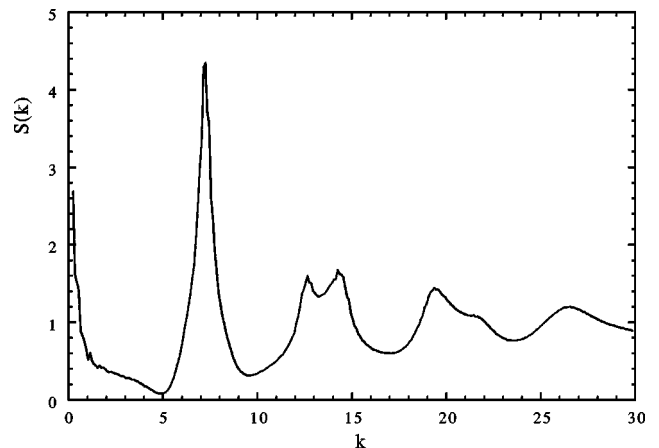

FIG. 5. Plot of the static structure function $S(k)$ at $T=2.7$ as a function of k. The height of the first diffraction maximum increases and its width decreases as T is lowered from $T=5.5$ (see Table I).
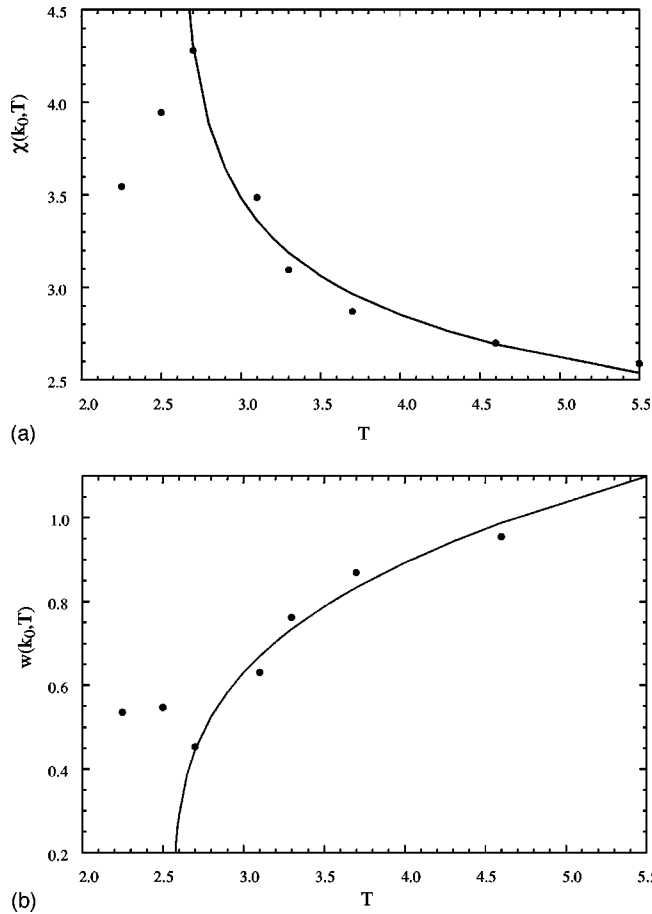
FIG. 6. (a) The temperature dependence of $\chi(k_0,T)$, the height of the diffraction peak of $S(k)$, at $k=k_0\approx7.15$. The solid line represents the best fit in the range $2.7\leq T\leq5.5$ and has the form $(T-2.6)^{-0.16}$. (b) The temperature dependence of $w(k_0,T)$, the width of the diffraction peak of $S(k)$. The solid line represents the best fit in the range $2.7\leq T\leq5.5$ and has the form $(T-2.6)^{0.29}$.
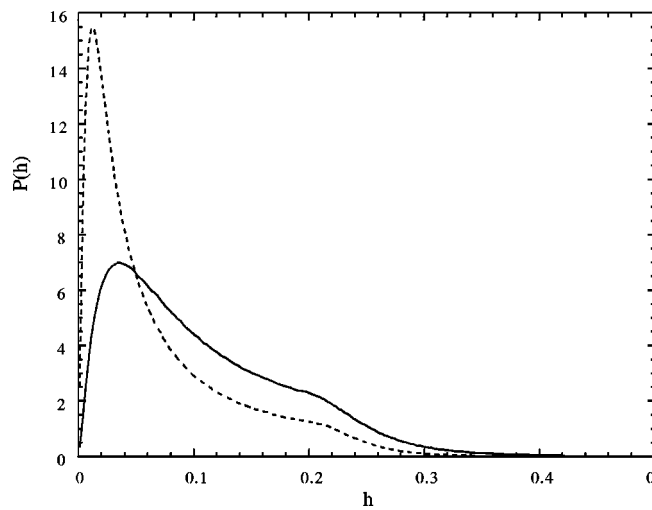

FIG. 7. Plot of $P(h)$, the estimated probability density of h, the relative variance of the edge length of the Voronoi polygons, at $T=5.5$ (solid line) and $T=2.7$ (dotted line). The data points are not shown to avoid confusion. Regular hexagons and hence lower values of h are much more likely at low temperatures. Note that $P(h)$ is not bimodal at any temperature. The shoulder in $P(h)$ at $h\approx0.25$ appears to be real rather than statistical error.
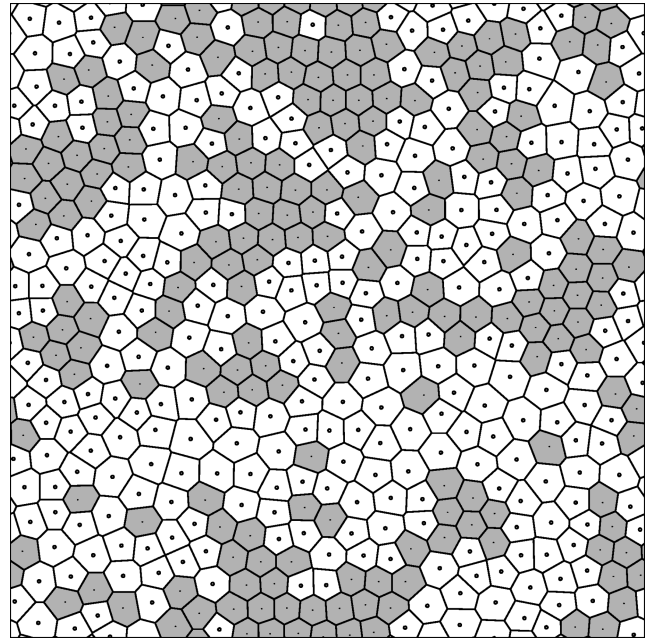

FIG. 8. A typical configuration at $T=3.3$ showing the Voronoi polygon for each particle and the clusters of the majority small particles (shaded hexagons).

the same order of magnitude as the duration of our runs. The fact that larger clusters require a longer time to reach equilibrium than smaller clusters has been found previously in temperature quenches of Ising models near the spinodal [18]. Our simulation results for n_s for lower values of T show similar behavior. We will discuss other estimates of the lifetime of the clusters in the following.

The behavior of n_s for $T=5.5$ is shown in Fig. 11. No evidence for simple power-law behavior is observed, but the s dependence of n_s is consistent with a fit to the assumed form, $n_s\propto s^{-x}e^{-s/m_s}$ with $x=1.1$, and $m_s=13$. Similar fits can be made for $T=4.7$ with $x=1.2$, and $m_s=21$, and $T=3.7$ with $x=1.4$, and $m_s=42$. We note that the effective value of the power-law exponent x and the cutoff parameter m_s increases as the temperature is decreased, suggesting that
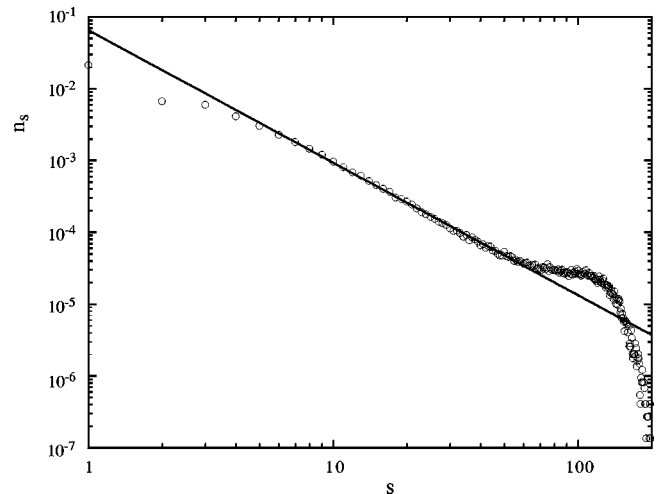

FIG. 9. Log-log plot of n_s, the cluster size distribution, versus size s at $T=3.3$ for $N=500$ particles. The solid line with slope $x=1.85$ is the best fit in the range $6\leq s\leq61$.
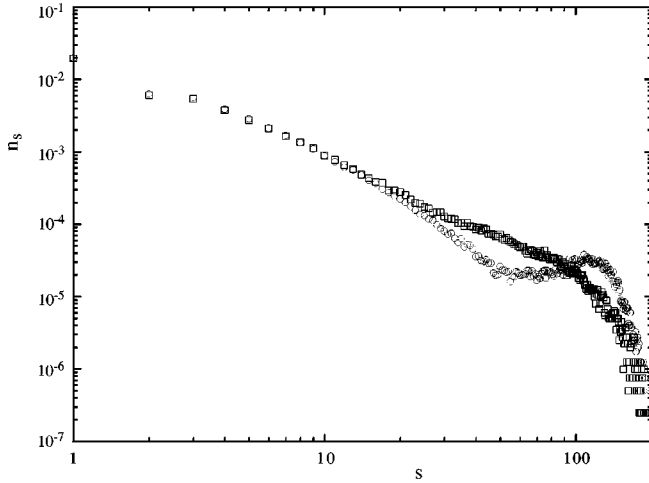
FIG. 10. Log-log plot of n_s versus s at $T=3.1$ for $N=500$ particles. The results for the first $50\,000\tau$ (open circles) and the second $50\,000\tau$ (open squares) are shown separately. The system was run for $50\,000\tau$ before data were taken. Note the difference in the size distribution of clusters for larger values of s.

a weak singularity is being approached.

Because our results for n_s for $N=500$ might be affected by finite size effects, we did a run for $N=20\,000$ particles at $T=2.7$ for a time of $30\,000\tau$. The system was run for $15\,000\tau$ before data were collected. A log-log plot of n_s versus s is shown in Fig. 12. It is clear that the values of n_s for larger s are not in equilibrium. However, a power-law fit of n_s in the range $4 \leq s \leq 61$ yields a slope of $x=1.75$, a value of x consistent with the value estimated from our results for $N=500$ at $T=3.3$.

We expect that if the clusters are important near the glass transition, their lifetime should increase as the glass transition is approached. As indicated in Fig. 10, we know qualitatively that the lifetime of the larger clusters becomes very long as the temperature is reduced. We introduce a measure of the cluster lifetime by measuring the time dependence of a metric associated with the solidlike particles. We divide the simulation cell into boxes and compute the number of solid-
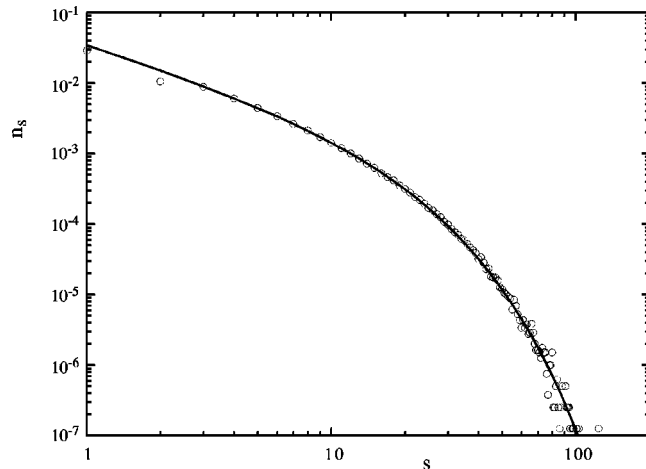

FIG. 11. Log-log plot of n_s versus s at $T=5.5$ for $N=500$ particles. The plot shows curvature indicating that there is not a simple scaling regime. The solid line is a fit to the form $n_s = As^{-x}e^{-s/m_s}$ with $A=0.038$, $x=1.1$, and $m_s=13$.
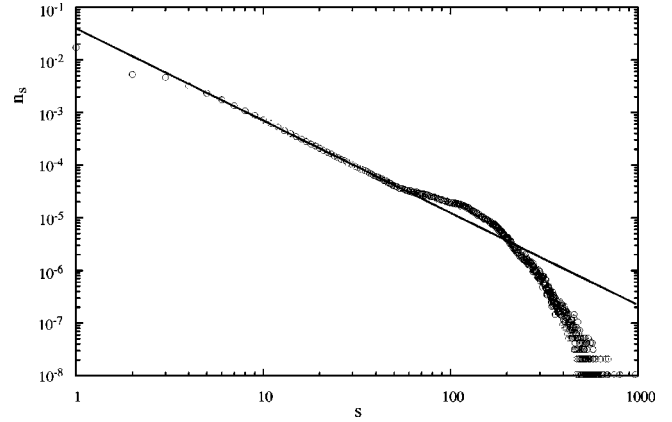

FIG. 12. Log-log plot of n_s versus s at $T=2.7$ for $N=20\,000$ particles. The linear fit was done for $5 \leq s \leq 61$ and yields a slope of $x=1.75$.

like particles in each box. The idea is to find if the time averaged number of solidlike particles in each box becomes the same when the time $t \gg 1$. We take n_α to be the number of solidlike particles in box α and compute the cluster fluctuation metric $\Omega_{cl}(t)$ defined as

$$\Omega_{cl}(t) = \frac{1}{N_b} \sum_{\alpha=1}^{N_b} [\bar{n}_\alpha(t) - \langle \bar{n}(t) \rangle]^2. \qquad (10)$$

In Eq. (10) $\bar{n}_\alpha(t)$ is the mean number of solidlike particles in box α at time t, and $\langle \bar{n}(t) \rangle$ is the mean occupancy averaged over all N_b boxes. For our runs we divided the system into 5×5 boxes. A linear increase in $1/\Omega_{cl}(t)$ defines the cluster mixing time τ_{cl} as in Eq. (7).

At $T=5.5$, $\Omega_{cl}(t)$ exhibits ergodic behavior with $\tau_{cl} \approx 500\tau$ [see Fig. 13(a)]. Our estimates for τ_{cl} for our runs are summarized in Table III. Note that for $T=3.1$ [see Fig. 13(b)], τ_{cl} is order $5 \times 10^4 \tau$, a time which is comparable to the duration of runs. For $T < 3.1$, our estimates of τ_{cl} are longer than the duration of our runs and are not meaningful. We interpret the time τ_{cl} as an estimate of the lifetime of the clusters. Note that at $T=3.1$, the times associated with the cluster lifetime and the motion of single particles differ by a factor of 10^3. The T dependence of τ_{cl} is best approximated by a Vogel-Fulcher form $\tau_{cl} \sim e^{C/(T-T_{cl})}$, where T_{cl} is the extrapolated temperature at which the cluster lifetime would become infinite. Although our estimates for τ_{cl} are only qualitative, the estimated value of T_{cl} found by considering the values of τ_{cl} in the range $3.1 \leq T \leq 5.5$ yields a reasonable fit with $T_{cl} \approx 1.6$ (see Fig. 14). This estimate of T_{cl} does not vary much if the results at $T=3.3$ and $T=3.7$ are omitted (see Table IV).

Another single particle decorrelation time can be extracted from $n_b(t)$, the number of unbroken Voronoi bonds remaining after a time t. At $t=0$, only Voronoi bonds between small particles that have exactly six small neighbors are counted. If at a time t later, there is no longer a bond which joins the same pair of particles, the number of bonds is reduced, and we do not consider this pair of particles again. We find that $\langle n_b(t)n_b(0) \rangle \sim e^{-t/\tau_b}$. Because a bond is broken every time a particle changes neighbors, we expect
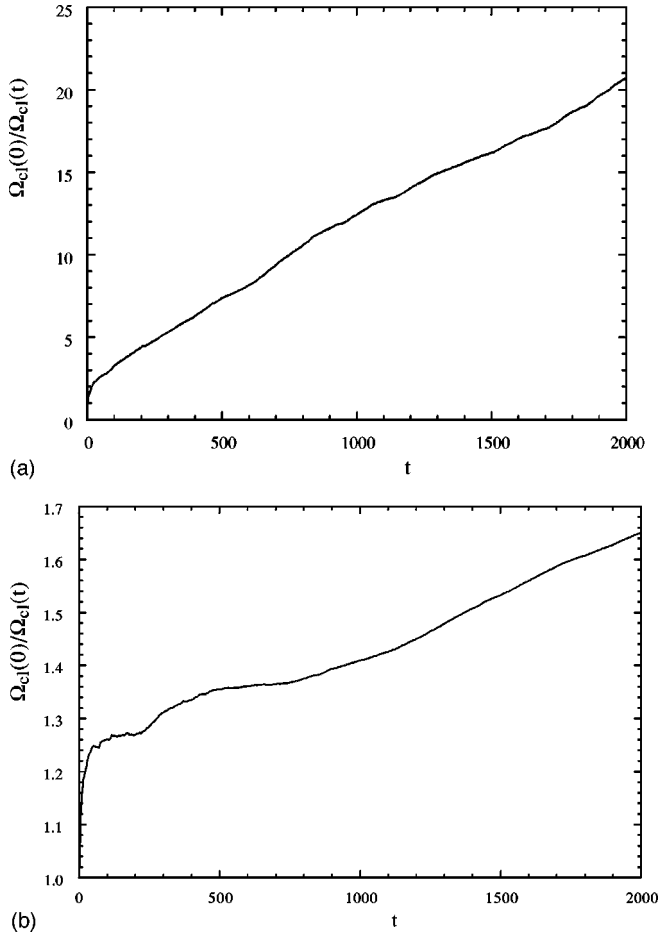
(a)

(b)

FIG. 13. The time dependence of $\Omega_{cl}(0)/\Omega_{cl}(t)$, where $\Omega_{cl}(t)$ is the cluster fluctuation metric defined in Eq. (10) at (a) $T=5.5$ and (b) $T=3.1$. Note the very different vertical scales in (a) and (b). The time t is given in terms of τ defined in the text.

FIG. 14. Plot of the cluster mixing time τ_{cl} (solid circles) versus T, where τ_{cl} is extracted from the linear time dependence of $1/\Omega_{cl}$. The solid line represents the best fit to the Vogel-Fulcher form $\tau_{cl}(T)=Ae^{C/(T-T_{cl})}$ with $A=19.8$, $C=11.8$, and $T_{cl}=1.58$ in the interval $3.1 \leq T \leq 5.5$.

that $\tau_b \sim \tau_D$. We computed τ_b for only a few temperatures and found that τ_b is comparable to τ_D.

Given the very long lifetime of the clusters for $T \leq 3.1$, it is difficult to make estimates of the errors associated with various quantities. For example, even though we made long runs at low temperatures, we found only one statistically independent configuration as far as the clusters are concerned. For this reason, quantities which are measures of the structure of the system, such as $S(k)$, are probably not adequately sampled for $T \leq 3.1$. And although our measures of single particle properties such as the velocity metric show the system to be ergodic at this level, the values of D at low T might also be inadequately sampled because the motion of the particles is influenced by the presence of the long-lived clusters.

It is not clear from our results and various fits whether we can identify one or two temperatures which can be associated with a glass transition. Our estimates for the temperature T_0 at which the self-diffusion coefficient vanishes and measures of the single particle properties become nonergodic are in the range $1 \leq T_0 \leq 2$. In comparison, our estimates for the temperature T_s at which the k-dependent susceptibility $\chi(k_0)$ and the inverse width $w^{-1}(k_0,T)$ would diverge if a spinodal were present are in the range $2.6 \leq T_s \leq 3.0$. The cluster distribution exhibits power-law scaling at a temperature
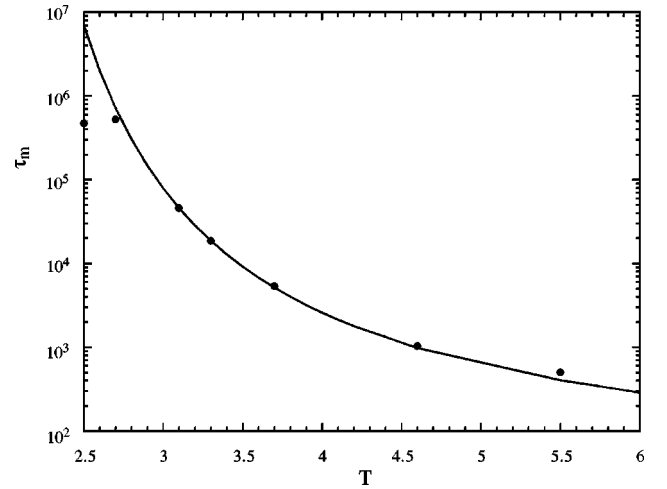
which is close, but not too close, to our estimate of T_s. At $T \approx 3.1$, the lifetime of our clusters is already comparable to the duration of our runs. Nevertheless, if we extrapolate the cluster lifetime to lower temperatures by fitting the cluster lifetime to a Vogel-Fulcher form, we find that the cluster lifetime becomes infinite at $T_{cl} \approx 1.6$, a temperature consistent with our estimate of T_0.

Given the small size of our system for all but one of our runs and the limited number of temperatures available, it is difficult to make quantitative conclusions in spite of the relatively long duration of our runs. Moreover, as we have emphasized, our interpretation of our molecular-dynamics data is justified only in the context of our rigorous results for the mean-field model of a structural glass discussed in Sec. I.

V. MEAN-FIELD INTERPRETATION AND SUMMARY

On the basis of our molecular-dynamics simulations, we can conclude that the deeply supercooled, two-component, two-dimensional Lennard-Jones system is heterogeneous. The heterogeneity can be characterized both dynamically and statically, that is, there are long-lived spatially correlated regions of all sizes up to a cutoff. This qualitative conclusion is consistent with the results of rotational diffusion experiments on probe molecules in supercooled o-terphenyl [19], which indicate that the dynamics in supercooled o-terphenyl is spatially heterogeneous, and with the results of other simulations [20].

An important question is the appropriate theoretical understanding of the origin of the spatial heterogeneity. In the future we plan to give a mean-field argument for the origin of the scaling behavior of the cluster size distribution in terms of an arrested nucleation picture [21].

We have found indirect evidence for mean-field behavior and the influence of a pseudospinodal. As discussed in Sec. II, the height of the diffraction peak of the static structure function $S(k)$ for the mean-field structural glass model exhibits a true divergence [5] in the limit $R \rightarrow \infty$. For finite-range R, the peak of $S(k)$ appears to diverge if it is measured

for values of the temperature T which are close, but not too close, to the apparent singularity and the data are extrapolated to lower T. However, a singularity in the peak of $S(k)$ is not observed if measurements are made too close to the apparent singularity. This behavior of $S(k)$ is characteristic of a pseudospinodal. Is there a spinodal in the Lennard-Jones system? The answer is no, because the range of the Lennard-Jones potential is finite. However, we found that the height and the inverse width of the diffraction peak of $S(k)$ exhibit a weak power-law divergence if their behavior is extrapolated from high T. This behavior is consistent with a pseudospinodal interpretation.

We expect that the Lennard-Jones system would be better described by mean-field theory as the density is increased, because the number of interactions each particle experiences increases. At present, we do not know how to calculate the effects of the pseudospinodal in dense Lennard-Jones systems [22], and we need to rely on simulations. Several other measurements suggest that the deeply supercooled, dense Lennard-Jones liquid can be described at least qualitatively by a mean-field picture. Glaser and Clark [23] found cluster scaling in a simulation of a two-dimensional Lennard-Jones system near the freezing transition. On the basis of a mean-field theory, it has been predicted that near the liquid-solid spinodal, the nucleating droplets are fractal-like rather than compact objects [24,25]. This effect has been observed in simulations of a three-dimensional Lennard-Jones system [26]. A third result consistent with a mean-field interpretation is that the measured value of the fractal dimension of the structures formed in a single-component two-dimensional Lennard-Jones system undergoing spinodal decomposition is consistent with that predicted by mean-field theory [15,27]. These results, together with the results reported here, suggest that a mean-field interpretation is applicable to dense Lennard-Jones systems under the proper conditions.

We note that although the clumps in the mean-field glass model and the solidlike clusters in the Lennard-Jones system have some properties in common, for example, their long lifetime, the clumps are not directly analogous to the clusters. As discussed in Ref. [28], the clump size distribution is a Gaussian in contrast to the power-law distribution that we found for the solidlike clusters. Although a theoretical definition of the clusters in the mean-field glass model does not exist, we can follow a similar approach and assume that a cluster in the latter system is a group of clumps such that each clump is in a triangular environment (in two dimensions). A preliminary investigation [28] of such a criterion for a cluster of clumps yields clusters which have a power-law distribution near the spinodal consistent with our results for the Lennard-Jones system.

Our argument for the association of the glass transition with an underlying thermodynamic transition is consistent with the recent interpretation by Nagel and co-workers [29] of the frequency dependence of $\epsilon''(\omega)$, the imaginary part of the dielectric susceptibility, in organic glass-forming liquids. Nagel and co-workers [29] have fitted $\epsilon''(\omega)$ to a single scaling curve over 13 decades of frequency for a wide range of T and for many glass formers. If the temperature dependence of the high frequency, power-law behavior of $\epsilon''(\omega)$ is extrapolated to lower frequencies, it is found that the static susceptibility diverges at a temperature T_σ with the corresponding mean-field exponent [30]. The magnetic susceptibility in dipolar-coupled Ising spin glasses is found to have similar behavior. Given that these experiments have been done on fragile glass-forming liquids with long molecules and on dipolar magnets, a mean-field interpretation of these results is consistent with our picture of the glass transition. That is, these systems are well approximated by mean-field models due to the large number of simultaneous interactions which each molecule has with its neighbors [31].

Our interpretation of our simulations in terms of an underlying thermodynamic transition in Lennard-Jones systems is consistent with the results of recent laboratory experiments. However, the interpretation of the single particle behavior in terms of a distinct kinetic transition is more open to question. Although such an interpretation is rigorous for our mean-field model of a structural glass, Menon and Nagel [30] have interpreted their experimental results in terms of a *single* glass transition temperature. That is, the temperature T_σ at which the static susceptibility is extrapolated to diverge is the same temperature at which the self-diffusion coefficient is extrapolated to vanish. In contrast, we find two distinct temperatures in the mean-field glass model and also can interpret our simulation results of the Lennard-Jones system in terms of two temperatures. We note that in the mean-field limit the number of particles in each clump is infinite, and the system would remain indefinitely in a local free energy minimum as determined by the number and location of the clumps. The duration of our simulations of the Lennard-Jones system is sufficiently short ($\approx 10^{-7}$ s) that at low temperatures the clusters do not diffuse and particles in the interior of the clusters are trapped. Moreover, the mean cluster lifetime near the glass transition is estimated to be an order of magnitude longer than our longest runs. This picture of static clusters is consistent with the mean-field model, but might not be appropriate for experimental time scales. Hence, it is possible that if we were able to run for longer times, we would find that the extrapolated temperature at which the self-diffusion coefficient vanishes and the extrapolated temperature of the underlying thermodynamic glass transition would approach each other.

Other workers have also interpreted the behavior of supercooled liquids near the glass transition in terms of clusters. Kivelson and co-workers [32] have proposed a thermodynamic theory of supercooled liquids based on the assumed existence of a ''narrowly avoided'' thermodynamic phase transition. The avoided transition is attributed to the existence of strain. In contrast to this transition, the spinodal transition always occurs below the first-order transition temperature. The reason that the spinodal transition is ''avoided'' in our interpretation is due to the fact that the system is not really mean field.

On the basis of our results for the temperature dependence of $w(k,T)$, the width of the first peak of $S(k)$, we can conclude that there is an increasing length scale which is associated with the clusters as the temperature is decreased. In our interpretation this increasing length scale is due to the effects of the pseudospinodal. This length scale would diverge if a spinodal were really present. The relation of this increasing length scale to the increasing maximum length scale for propagating transverse current correlations observed by Mountain [33] requires further study. In contrast,
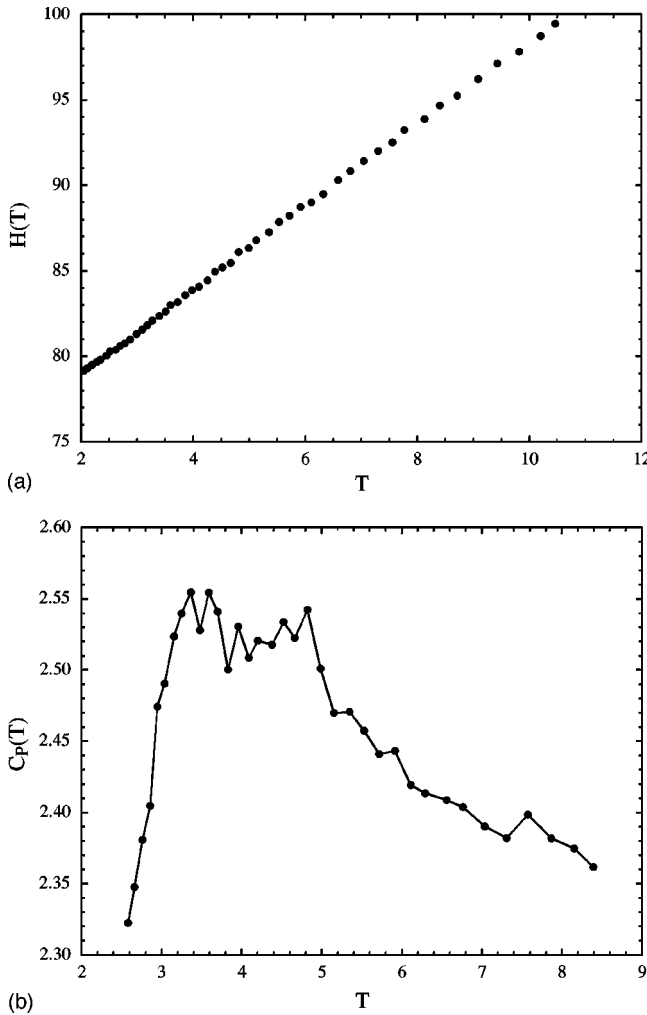
FIG. 15. The temperature dependence of the (a) (dimensionless) enthalpy H and (b) the heat capacity C_P at $P = 70$. Note that C_P has a small peak at $T \approx 4$. As explained in the text, the slope of $H(T)$ was computed at each value of $T = T_i$ and the value of C_P at $T = T_i$ was computed by doing a least squares fit to 15 successive slopes in the interval $T_{i+7} - T_{i-7}$.

though the pseudospinodal has measurable effects including increasing length and time scales as the pseudospinodal is approached. In addition to this glass-pseudospinodal transition, there is a temperature (for fixed density) which can be interpreted as a kinetic transition below which the self-diffusion coefficient is not measurable during our observation time.

We are presently simulating much larger Lennard-Jones systems in two dimensions to obtain better statistics for the clusters over a wider range of sizes and over a range of temperatures above the glass transition. If our mean-field interpretation is correct, we should be able to observe similar behavior in three dimensions where mean-field behavior should be even more apparent. However, the identification of the clusters in three dimensions is not straightforward because of the existence of a variety of possible local symmetries which are more affected by thermal fluctuations than in two dimensions.

APPENDIX: THE ENTHALPY

Many computer simulations of glasses show that the heat capacity C_P has a maximum in the vicinity of the glass transition. For example, Wahnström [35] has computed the temperature dependence of the energy of a two-component, three-dimensional Lennard-Jones system and has found that the slope changes at a temperature where the dynamical anomalies are most pronounced. In the following, we discuss our measured values of the temperature dependence of the enthalpy H.

We measured H using constant pressure molecular dynamics [36] for $N = 500$ particles. The system was equilibrated at $T \approx 10$ and a series of measurements of H were performed at progressively lower temperatures spaced approximately 0.02 apart for the higher values of T and approximately 0.01 apart at the lower values of T. At each value of T, the system was equilibrated for 250τ and H was averaged over the following 250τ. These runs are relatively short in comparison to the runs reported in the main text.

Our results at $P = 70$ for H and C_P are shown in Fig. 15. A careful inspection of $H(T)$ shows that its slope changes as a function of T. Note that $C_P(T)$ increases as T is lowered, reaches a maximum at $T \approx 4$, and decreases as T is lowered further. The slope of $H(T)$ was computed as each value of $T = T_i$ from the numerical derivative, $[H(T_{i+1}) - H(T_i)]/[T_{i+1} - T_i]$. The values of $C_P(T = T_i)$ shown in Fig. 15 were computed by doing a least squares fit to 15 successive slopes in the interval $T_{i+7} - T_{i-7}$. If we consider fewer than 15 points, the results for $C_P(T)$ were too noisy. The results for more than 15 points tended to smooth the peak in C_P.

an increasing correlation length was not observed in a simulation [34] of the translational and orientational correlation functions of a two-component three-dimensional Lennard-Jones system.

The effects of the pseudospinodal and the incipient thermodynamic glass transition will be more or less apparent depending on the interaction range, the details of the interaction, and the spatial dimension [7]. We do not expect to find spinodal-like effects in all supercooled liquids. These considerations suggest that there is a class of materials for which the observed glass transition is associated with a pseudospinodal and an incipient thermodynamic transition, and other materials for which the observed glass transition might not be associated with such effects.

Based on our Monte Carlo and theoretical studies of a mean-field model and our molecular-dynamics results for a two-dimensional Lennard-Jones system, we suggest that the latter is in the class of systems whose behavior can be attributed to an incipient thermodynamic instability (the pseudospinodal). We emphasize that a true thermodynamic glass transition does not exist in the Lennard-Jones system, even

We note that the spinodal singularity in the mean-field glass model is at $k = k_0 \neq 0$, and hence we do not expect thermodynamic quantities such as C_P to exhibit a divergence at the spinodal in the mean-field limit. However, for a system that does not exhibit a true spinodal such as the present Lennard-Jones system, it is possible that the coupling between the $k = k_0$ and $k = 0$ modes might lead to a maximum in quantities such as C_P near the pseudospinodal.

[1] Reviews of the properties of structural glasses can be found, for example, in *Liquids, Freezing, and the Glass Transition*, edited by J. P. Hansen, D. Levesque, and J. Zinn-Justin (North-Holland, Amsterdam, 1991); W. Götze and L. Sjögren, Rep. Prog. Phys. **55**, 241 (1992); R. D. Mountain, Int. J. Mod. Phys. C **5**, 247 (1994); C. A. Angell, Science **267**, 1924 (1995); *Glasses and the Glass Transition*, edited by S. C. Glotzer, special issue of Comput. Mater. Sci. **4**, 283 (1995); M. D. Ediger, C. A. Angell, and S. R. Nagel, J. Phys. Chem. **100**, 13 200 (1996).

[2] A. I. Mel'cuk, R. A. Ramos, H. Gould, W. Klein, and R. D. Mountain, Phys. Rev. Lett. **75**, 2522 (1995).

[3] W. Klein, H. Gould, R. Ramos, I. Clejan, and A. Mel'cuk, Physica A **205**, 738 (1994).

[4] M. Kac, G. E. Uhlenbeck, and P. C. Hemmer, J. Math. Phys. **4**, 216 (1961).

[5] N. Grewe and W. Klein, J. Math. Phys. **18**, 1729 (1977): **18**, 1735 (1977).

[6] R. A. Ramos, Ph.D. thesis, Boston University, 1994.

[7] D. W. Heermann, W. Klein, and D. Stauffer, Phys. Rev. Lett. **49**, 1262 (1982).

[8] M. A. Novotny, W. Klein, and P. Rikvold, Phys. Rev. B **33**, 7729 (1986); and M. A. Novotny, P. Rikvold, and W. Klein (unpublished).

[9] I. Clejan, Ph.D. thesis, Boston University, 1994.

[10] D. Thirumalai and R. D. Mountain, Phys. Rev. E **47**, 479 (1993); R. D. Mountain and D. Thirumalai, Physica A **210**, 453 (1994). In this context a system is ergodic if time averages and ensemble averages are equal.

[11] Y. J. Wong and G. V. Chester, Phys. Rev. B **5**, 3506 (1987).

[12] See for example, H. Gould and J. Tobochnik, *Introduction to Computer Simulation Methods*, 2nd ed. (Addison-Wesley, Reading, MA, 1996); or D. Rapaport, *The Art of Molecular Dynamics Simulation* (Cambridge University Press, Cambridge, England, 1996).

[13] A. I. Mel'cuk, Ph.D. thesis, Clark University, 1994.

[14] A. Coniglio and W. Klein, J. Phys. A **13**, 2775 (1980).

[15] W. Klein, Phys. Rev. Lett. **65**, 1462 (1990).

[16] R. E. M. Moore and I. O. Angell, J. Comput. Phys. **105**, 301 (1993).

[17] N. N Medvedev, A. Geiger, and W. Brostow, J. Chem. Phys. **93**, 8337 (1990).

[18] L. Monette and W. Klein (private communication); D. Stauffer (private communication).

[19] See, for example, M. T. Cicerone and M. D. Ediger, J. Chem. Phys. **103**, 5684 (1995).

[20] R. D. Mountain, in *Symposium Series No. 676, Supercooled Liquids: Advances and Novel Applications*, edited by J. Fourkas, D. Kivelson, K. Nelson, and U. Mohanty (American Chemical Society, Washington, D.C., 1997), Chap. 9; W. Kob, C. Donati, S. J. Plimpton, P. H. Poole, and S. C. Glotzer, Phys. Rev. Lett. **79**, 2827 (1997).

[21] W. Klein *et al.* (private communication).

[22] R. Lovett, J. Chem. Phys. **66**, 1225 (1977).

[23] M. A. Glaser and N. A. Clark, Adv. Chem. Phys. **83**, 543 (1993), use sixfold bond orientational order to define the clusters in a one-component, two-dimensional Lennard-Jones system.

[24] W. Klein and C. Unger, Phys. Rev. B **28**, 445 (1983); C. Unger and W. Klein, *ibid.* **29**, 2698 (1984).

[25] W. Klein and F. Leyvraz, Phys. Rev. Lett. **57**, 2845 (1986).

[26] J. Yang, H. Gould, W. Klein, and R. Mountain, J. Chem. Phys. **93**, 711 (1990).

[27] R. C. Desai and A. R. Denton, *Growth and Form*, edited by H. E. Stanley and N. Ostrowsky (Martinus Nijhoff Press, Dordrecht, 1986).

[28] L. Colonna-Romano (unpublished).

[29] P. K. Dixon, L. Wu, S. R. Nagel, B. D. Williams, and J. P. Carini, Phys. Rev. Lett. **65**, 1108 (1990).

[30] N. Menon and S. R. Nagel, Phys. Rev. Lett. **74**, 1230 (1995).

[31] K. Binder, Phys. Rev. A **29**, 341 (1984).

[32] S. A. Kivelson, A. Zhao, D. Kivelson, T. M. Fischer, and C. M. Knobler, J. Chem. Phys. **101**, 2391 (1994); D. Kivelson, S. A. Kivelson, X. Zhao, Z. Nussinov, and G. Tarjus, Physica A **219**, 27 (1995).

[33] R. D. Mountain, J. Chem. Phys. **102**, 5408 (1995).

[34] R. M. Ernst, S. R. Nagel, and G. S. Grest, Phys. Rev. B **43**, 8070 (1991).

[35] G. Wahnström, Phys. Rev. A **44**, 3752 (1991).

[36] H. C. Andersen, J. Chem. Phys. **72**, 2384 (1980).